HEAT TRANSFER TO A SEEDED FLOWING GAS FROM AN ARC ENCLOSED BY A QUARTZ TUBE

by Chester D. Lanzo and Robert G. Ragsdale
NASA Lewis Research Center,
Cleveland, Ohio

ABSTRACT

Experimental results are presented for combined radiation and forced-convection heat transfer to air containing submicron carbon particles flowing in the annulus of a transparent heat exchanger. The heat exchanger is 14 inches long; it is composed of two concentric quartz tubes, one 2 inches in diameter and the other 3 inches. The heat source is an electric arc contained within the inner tube and stabilized by the vortex-type flow of nitrogen gas. Characteristic current-voltage curves established for arc lengths of 18 and 28 inches are shown to be consistent with, and extend the range of, previous data. Measurements obtained for arc powers from 125 to 280 kilowatts show that the fraction of arc power released as radiation increases from 12.5 percent to an apparent asymptote of about 20 percent. For arc power levels from 126 to 167 kilowatts, an overall heat balance within ±10 percent was obtained by accounting for the nitrogen enthalpy rise, convection, conduction, and radiation losses, and electrode cooling. The measured transmissivity of 0.027-micron-diameter carbon particles gave an extinction cross section of 22,800 square centimeters per gram compared with 121,000 square centimeters per gram estimated from Mie scattering theory. The fact that the present data are higher than previous measurements of 3030 square centimeters per gram is attributed to more effective particle dispersion. The seed-injection system used to disperse the particles in the air stream is described.

Heat-exchanger performance is presented in terms of the fraction of total heat transfer to the seeded air that is due to absorption of radiant energy. For seeded gas absorptivities from 0.09 to 0.3, the radiative transfer fraction varied from 0.13 to 0.40.

It is concluded that (1) a quartz-tube-contained electric arc is an effective device for radiation heat-transfer studies and that (2) the addition of a small amount of solid particles to a flowing transparent gas can significantly increase the total heat transfer in a system where both forced convection and radiation heat sources are present.

INTRODUCTION

Early interest in radiation heat transfer was primarily associated with industrial applications, such as furnaces, and was thus mainly concerned with radiant interchange between solid surfaces and absorbing gases, such as carbon dioxide and water vapor. More recently, the advent of plasma generators, reentry missiles, and gaseous nuclear rocket concepts has greatly increased interest in combined radiative and convective heat-transfer processes. Most of these applications give rise to analytically complex two-dimensional problems involving radiation, convection, and conduction heat transfer to absorbing and emitting gases. In general, this class of problems leads to a set of nonlinear integrodifferential equations that cannot be solved simply.

One-dimensional solutions have been obtained[1,2,3,4] for a gray gas (i.e., one whose absorption coefficient is independent of both wavelength and temperature). Application of Monte Carlo statistical methods to nongray gas radiation has also been investigated for a stagnant gas.[5] A two-dimensional finite-difference solution of the exact integrodifferential equations has been obtained for a gray gas with conduction and gas flow between parallel flat plates[6] and through a circular pipe.[7] Reference 7 also includes the effect of internal heat generation in the absorbing gas.

The analysis of reference 7 has been applied to a nuclear propulsion system wherein the energy is radiatively transferred from a fissioning gas to a nontransparent propellant flowing in a surrounding annulus.[8] In this particular application (nuclear propulsion) the "nontransparent" propellant is hydrogen, a gas normally transparent below about 15,000° R, that has been seeded with small particles, liquid droplets, or another gas. The nontransparent behavior of gases containing small particles is also of interest in combustion processes (flame emissivity)[9] and atmospheric attenuation of solar radiation.

Though some experimental work has been reported on fluid-solid systems, there is little at conditions where radiation contributes significantly to the temperature rise of a flowing gas. Turbulent forced-convection heat transfer to a fluid-solid mixture has been studied[10] as well as furnace heating of solid particles.[11] The transmission properties of small particle clouds have been measured[12] for a limited range of conditions, but theory remains the primary source of both optical[13,14] and fluid mechanical[15,16] properties of gas-solid systems.

The investigation described in this paper is one of a flowing transparent gas seeded with small particles and exposed to simultaneous conduction and radiation heat transfer. Since both the heat-transfer and optical characteristics of such a system are incompletely understood, the approach has been experimental. From an experimental viewpoint, the principal consideration was one of the physical system. It had to provide a source of both radiation and conduction heating of the flowing gas-solid stream. These conditions do not exist in the usual heat transfer devices that involve flow over or between solid surfaces. Because of the temperature limitation imposed by the heated surface, essentially all of the energy transfer is by conduction regardless of the opacity of the fluid.

The experimental device used in this study was a transparent heat exchanger composed of two concentric quartz cylinders. Air containing submicron carbon "dust" passed through the annular region and was heated by conduction from and radiation through the inner quartz tube. The heat source was an electric arc stabilized by the vortex-type flow of nitrogen gas within the inner tube. The primary objective was to utilize a heat exchanger that would provide a significant fraction of the total heat transfer in the form of radiation. In other words, the arc was not under study per se; the glass tube containing the arc was simply a source of radiant energy. Since this particular application of an electric arc was relatively unique, a certain degree of attention was necessarily directed to those arc characteristics relating to energy radiation.

The overall purpose of this investigation, then, was twofold: First, it was desired to evaluate the characteristics and usefulness of an electric arc as a research device with which to study radiation heat transfer. The second goal was to obtain some experimental data on the relative increase of heat transfer caused by the addition of small solid particles to a normally transparent gas in a system where both forced convection and radiation are possible modes of heat transfer.

EXPERIMENTAL APPARATUS

Arc Source

Figure 1 shows a schematic drawing of the experimental apparatus and most of the instrumentation employed in the investigation. With the exception of the power supply, the basic arc setup is the same as that described in reference 17.

The arc is contained in a 54-millimeter (O.D.) quartz tube having a wall thickness of 4 millimeters. Tube lengths of 18 and 28 inches were used. The arc is maintained between fixed-upstream and movable-downstream water-cooled copper electrodes. The arc is stabilized by metered nitrogen gas that is introduced through a vortex generator at the fixed-electrode end. The nitrogen exhausts into an insulated collector where it is mixed with ambient air. The grounded downstream electrode is mounted on a movable carriage. The arc is initiated by a pneumatic electric servosystem that drives the downstream electrode into the quartz tube until contact is made with the fixed electrode. Then the movable electrode is withdrawn to a position 2 inches beyond the end of the quartz tube. The entire starting sequence is accomplished in about 10 seconds.

The variable-frequency alternating-current power supply available provided continuous variation of voltage from a minimum of 540 up to 6480 volts with an associated frequency of 1 cycle per second for each 54 volts. A maximum power of 7 megawatts was available at the limiting current of 1125 amperes. A bank of water-cooled stainless-steel tubing was used as a 1.6-ohm pure resistance in series with the arc to provide electrically stable operation.

Transparent Heat Exchanger

The parallel flow quartz heat exchanger is shown in figure 2. The outer quartz tube is 84 millimeters (O.D.) and the heat exchanger is 14 inches long. The nitrogen vortex generator can be seen on the left of the figure. The exhaust gas collector normally surrounding the downstream electrode is not shown. Mounted behind the heat exchanger are thermocouples in contact with the outer quartz tube. Additional cooling air is provided by the three tubes running parallel to the heat exchanger.

Seeded air is introduced into the annulus of the heat exchanger through an entrance nozzle attached to the front of the vortex generator. The air flow is metered with a rotameter before the carbon particles are added to it. The mixture passes through the heat exchanger and is then exhausted to a vacuum system. The pressure in the heat exchanger was maintained at 1 atmosphere.

Particle Injection System

Commercially available particle-injection devices are designed to handle relatively large particles - 50 microns in diameter and larger - and did not perform satisfactorily with the submicron carbon dust employed in these tests. At best, they injected particle agglomerations and, at worst, did not function at all. For this reason, an injection system was designed specifically for the submicron particles used.

Figure 3 is an electronphotomicrograph at a magnification of 130,800 of the carbon particles used in the tests. The particle indicated by the arrow is assumed to be representative of the average size; 0.027 micron in diameter. The larger clumps in the photo appear to be particle agglomerates rather than single particles. The fact that the particle images in the figure are circular suggests that the actual particles were spherical in shape. It is assumed then

that the particles used in the tests can be characterized as being 0.027-micron-diameter spheres. It should be pointed out that the condition of the particles shown is the result of electron microscope slide preparation procedure, and does not necessarily represent the degree of particle dispersion during the heat-exchanger tests.

Basically, the seeding apparatus consisted of a cylindrical powder container that was fitted with a piston plunger at one end. The plunger was driven at a preselected constant rate by a motor-operated screw assembly. The other end of the cylinder was attached to a vortex generator. The particles were introduced into the air stream, and the mixture entered the vortex chamber through an adjustable-height injection-slit nozzle. The choked-flow nozzle subjected the particle-air mixture to a severe pressure gradient. The mixture then passed through the vortex cavity where the resulting aerodynamic shear forces tended additionally to break up any remaining particle agglomerates. The particle-air mixture was exhausted through a centrally located hole in one face of the vortex chamber. The variable-height injection nozzle and variable plunger speed enabled operation over a wide range of conditions. Subsequent analysis of experimental data indicated that the injection system did tend to break up particle agglomerates in the air stream.

Instrumentation

The primary measurements made during a test run were:

(1) Air and nitrogen flow rates

(2) Air and nitrogen inlet and outlet temperatures

(3) Radiation intensity from arc

(4) Particle injection rate

(5) Arc voltage and current

Air and nitrogen flow rates were measured with a rotameter and an orifice, respectively. The nitrogen exhaust mixture and the air outlet temperatures, for both seeded and unseeded runs, were measured with a high stagnation, aspirated, radiation-shielded thermocouple. Maximum temperature corrections, though not used in data reduction, for this type of thermocouple are 10° F for radiation and 20° F recovery correction at a Mach number of 0.4 and 3350° R. The arc nitrogen outlet temperature was too high to be measured directly, so it was drawn into an insulated collector, along with some ambient air, and the lower temperature of the mixture was measured. The mass flow rate of the mixture was measured with an orifice downstream of the exhaust collector. The nitrogen outlet temperature was then calculated from the known values of mixture flow rate and temperature, ambient temperature, and nitrogen flow rate.

A thermopile radiation detector was used to measure the intensity of the emitted arc energy. It was mounted normal to the heat exchanger on a motor-driven assembly to permit both horizontal and vertical traverses. The detector was fitted with a glass tube 52 millimeters in diameter and 12 inches long to prevent stray radiation from influencing local readings. The inner surface of the tube was blackened, and there was a 1-inch-diameter opening in the exposed end. The thermopile output signal was recorded on a millivolt strip-chart recorder, and, when traverses were made, on an X-Y plotter.

The weight rate at which carbon particles were added to the air stream was

determined gravimetrically. The seed container was weighed before and after each run, and the time that the seed injector was operated was measured. A seed charge was of the order of 30 grams, and a typical injection time was between 1 and 2 minutes.

The electrical power delivered to the arc was determined from measured values of arc current and voltage. Actual measurements were made on the secondaries of current and voltage transformers. Wave forms for a 24-cycle arc are shown in figure 4 as reproduced from traces on a dual-beam oscilloscope. The voltage shape is typically nonsine wave. The indicated voltmeter reading was checked for one run and found to be within 3 percent of the value given by a "true rms" meter. In addition, graphic integration of an instantaneous power curve obtained from the curves of figure 4 gave an average power within 5 percent of $E_{rms} \cdot I_{rms}$. So, it was considered to be satisfactorily within experimental error to obtain arc power directly from panel meter indications of voltage and current. A similar conclusion was reached in reference 17.

EXPERIMENTAL PROCEDURE

During operation, the arc facility was controlled from an adjoining room, and all data were remotely indicated and recorded. The arc was visually observed through a window of 1/4-inch-thick number eight welding glass.

Prior to arc ignition, electrode and ballast cooling water, and nitrogen and heat-exchanger air flows were established. The automatic-electrode drive sequence inserted the downstream electrode and, after strike, withdrew it to a position 2 inches beyond the end of the inner quartz tube. The desired power level was obtained by adjusting the voltage from the power supply. All readings were first taken with no carbon particles in the air stream. After steady-state conditions were observed, the seed injector was turned on for about 1 to 2 minutes. Figure 5 illustrates the time variation of primary measurements for a run and shows that steady-state conditions are rapidly achieved.

DISCUSSION OF RESULTS

Arc Characteristics

Although the basic arc apparatus is essentially the same as the one described in reference 17, the power supply and series resistance were different. This resulted in operation at lower voltages and considerably higher currents. Thus, it was possible to extend the range of data on the characteristic voltage-current curve of a nitrogen-vortex stabilized arc (see fig. 6). The bulk of the data from reference 17 were obtained for an arc length of 33 inches. The two points for arc lengths of 28 and 18 inches were taken from figure 18 of reference 17. The present data for arc lengths of 28 and 18 inches are consistent with, and extend the range of, the data of reference 17.

The primary effect of increasing arc current and power is to increase the radiative power of the arc.[18] For the nitrogen stabilized arc described in reference 17, measurements showed[19] that as arc power increased from 50 to 100 kilowatts, the percent of input energy released as radiation increased from 4.5 to 10 percent (see fig. 7). The data of this report show that as arc power is further increased to 300 kilowatts, the percent of power radiated continues to increase up to an apparent asymptotic value of about 20 percent. Both the data of this report and that of reference 18 can be represented by a single line with a deviation of ±10 percent.

The intensity of the emitted radiation was measured with a thermopile de-

tector located approximately 13 inches from the outer surface of the heat exchanger. The detector was situated halfway down the length of the exchanger; such a reading was assumed to be representative of the total radiation. An axial survey was made of the radiation intensity to check the validity of this assumption. Figure 8 shows that the radiation intensity is relatively independent of axial position over the length of the annular heat exchanger, for both seeded and unseeded air. The intensity increase beyond the exit end of the heat exchanger is caused by direct radiation from the arc.

The electrical power delivered to the arc is dissipated by a number of mechanisms. As was shown in figure 7, about 10 to 20 percent of the input power is transmitted through the quartz tube as thermal radiation. Other modes of energy consumption are (1) electrode cooling losses, (2) energy carried out by the nitrogen discharging from the inner quartz tube, (3) conduction from the hot quartz surface to the air flowing in the annulus, and (4) free convection from the outer quartz tube to the environment. The distribution of arc power is shown in figure 19 for eight runs of increasing power level. The electrical power input is also shown for each run. A typical distribution of arc power is given in Table I for run 7.

Table I. - Arc Power Distribution

Nitrogen exhaust	53 percent
Radiation	20 percent
Electrodes	19 percent
Conduction	7 percent
Free convection	1 percent

Although more than half of the input power is carried away by the nitrogen required to stabilize the arc, a significant portion, 20 percent, is available as thermal radiation. For this run, the 20 percent represents 33 kilowatts. This total amount of radiation includes 6 kilowatts radiated from the arc beyond the end of the heat-exchanger annulus. The 27 kilowatts radiated within the heat exchanger results in a radiant heat flux at the surface of the inner quartz tube of 305 watts per square inch. The total heat flux from the inner tube, including conduction, was 436 watts per square inch. For comparison, a radiant heat flux from a blackbody at 3050° R is 305 watts per square inch.

An overall heat balance on the arc can be obtained by comparing the total power accounted for with the input power. This is shown in figure 10; the heat balance is within ±10 percent. The largest source of error is introduced by the nitrogen exhaust temperature, a quantity that was not measured directly. The method of data reduction and the numerical calculations are given in the appendix for run 7.

Extinction Cross Section of Carbon Particles

The transmissivity, or ratio of transmitted to incident energy I/I_o, was obtained by measuring the radiation intensity from the arc with and without carbon particles in the air stream. The variation of transmissivity with the product of particle density times path length is shown in figure 11. The solid line drawn through the data is between those given by (1) Mie scattering theory[13] and (2) previous measurements of carbon particles dispersed in water.[12]

The physical significance of the data shown in figure 11 can be interpreted more clearly in terms of the particle cross section. The equation of a straight line on the semilog coordinates of figure 11 can be written in the form

$$I/I_o = e^{-\epsilon l_s} = e^{-E\rho_s l_s}$$

where ρ_s is the particle density (gm/cm^3), l_s is the path length through the particle system (cm), E is the extinction cross section per gram (cm^2/g), and ϵ is the extinction coefficient (cm^{-1}). The extinction cross section per gram E is the slope of the lines shown in figure 11, and, in general, is a function of particle material and the ratio of particle size to radiation wavelength.[13]

The variation of the extinction cross section per particle ϵ/N of carbon particles with particle size is shown in figure 12. Theoretical values* taken from references 13 and 14 are shown, as well as the geometric cross section. The data of this report are less than theoretical values but are considerably higher than the measurements of carbon particles dispersed in water. The relative values of extinction cross sections per particle and per gram are summarized in Table II.

Table II. - Extinction Cross Sections of

0.027-Micron-Diameter Carbon Particles

Source	E, cm^2/g	ϵ/N, cm^2/particle
Mie theory	121,000	200×10^{-14}
Present data	22,800	**38×10^{-14}
Ref. 12	3,030	**5×10^{-14}

The fact that the present data are higher than previous measurements and closer to theoretical estimates is attributed to better particle separation. It is felt that the extinction cross section data indicate that the particle injection system reduces particle agglomeration. Obviously, there are many factors involved in data such as these, but the conclusion seems justified. Further studies of particle size distribution, wavelength, and temperature effects are necessary to disclose whether complete particle separation exists.

Heat Exchanger Performance

The two parameters varied during the heat-exchanger tests were the arc power level and the carbon particle seeding density. Electrical power to the arc was varied from 126 to 167 kilowatts, with a corresponding range of heat transferred to the seeded air from 12.9 to 17.5 kilowatts. For all runs, the air flow rate was 0.095 pound per second. Carbon particle seeding density was varied from 5×10^{-6} to 10.5×10^{-6} gram per cubic centimeter; this corresponded to a weight percent in air from 1.17 to 2.43 percent.

For each power level, the heat transferred to the air stream was measured first without and then with carbon particles in the air stream. The heat transferred by radiation alone was obtained by subtracting the heat conducted to the

*The curve from reference 13 is the total extinction cross section, but for a 0.027-micron-diameter particle the scattering cross section is 1000 cm^2/gm - less than 1 percent of the total.

**In order to present the data as an extinction cross section per particle, it is necessary to calculate the number of particles that were present; in this calculation, it is assumed that there was no agglomeration. An equivalent assumption is made in the calculation of the theoretical cross section per gram.

unseeded air from the total heat transferred to the seeded air. This assumption that conduction and radiation are independent and additive processes should introduce an error less than 9 percent.[6]

The results are presented in terms of a radiative transfer fraction, or the fraction of total heat transfer that occurred by radiation, and the gas absorptivity, or fraction of incident radiation, that is absorbed. Figure 13 shows that for absorptivities from 0.09 to 0.3, the fraction of total heat transfer due to radiation increased linearly from 0.13 to approximately 0.4. It should be noted that even if the absorptivity were 1.0, the radiative transfer fraction would be less than 1.0, since some conduction heat transfer will always occur. For the conditions of run 7, for example, if all the radiated heat were absorbed by the air, the radiative transfer fraction would be 0.7.

A more general presentation of the effect of seeding on heat transfer is given in figure 14, where the Nusselt number ratio, seeded to unseeded air, is shown as a function of the particle density. In terms of the radiative transfer fraction, the Nusselt number ratio is given by

$$\frac{Nu'}{Nu} = \left(\frac{1}{1 - q_R/q_T}\right)\left[\frac{1 - T_B/T_S}{(1 - T_B/T_S)'}\right]$$

where T_B/T_S is the usual bulk-to-surface-temperature ratio, and the prime superscript indicates seeded air. The radiative transfer fraction q_R/q_T and the bulk temperature are measured quantities. The surface temperature T_S of the inner glass tube was not measured but can be reasonably estimated to be near but less than its softening point. It was assumed to be at 2000° F. For run 7, an error of 10 percent in the assumed surface temperature changed the Nusselt number ratio by less than 1.3 percent. Figure 14 shows that combined radiation-convection heat transfer to air seeded with less than 3 weight percent of carbon particles exceeds by about 65 percent that due to forced convection alone.

CONCLUSIONS

A heat-transfer experiment in a transparent heat exchanger constructed from two concentric quartz tubes was conducted. The heat source was an electric arc contained in the inner tube and stabilized by the vortex-type flow of nitrogen gas. Air flowing through the annular region was made absorptive to thermal radiation by the addition of submicron carbon particles. Measurements of the heat transfer to the air were made for air flowing with and without carbon particles. For arc power levels from 126 to 167 kilowatts and carbon-particle seeding from 1 to 2.5 weight percent, the following conclusions were indicated:

1. A quartz-tube-contained electric arc is a useful research device for radiation heat transfer studies. A radiation flux of 305 watts per square inch was obtained at the surface of a 54-millimeter-diameter tube; this is the radiant flux that would be emitted by a 3050° R blackbody surface.

2. An extinction cross section of 22,800 square centimeters per gram is attainable with 0.027-micron-diameter carbon particles. This is less than the Mie theoretical value of 121,000 but greater than a previously measured value of 3030. The optical properties of a particle-gas system are strongly affected by particle agglomeration. The increase of the present data over the previous values is attributed to reduced particle agglomeration achieved by injecting the mixture through a choked-flow nozzle into a vortex chamber.

3. The addition of a small weight fraction of solid particles to a flowing

transparent gas can significantly increase the total heat transfer in a system where both forced convection and radiation heat sources are present. For example, a 65-percent increase in heat transfer was obtained by adding less than 3 weight percent of carbon particles to an air stream flowing parallel to a quartz tube containing an electric arc.

ACKNOWLEDGEMENT

The authors gratefully acknowledge the considerable cooperation and assistance of the personnel of the Thermomechanics Research Laboratory of the Aerospace Research Lab, Wright-Patterson Air Force Base. They furnished the basic design of the arc facility used in this study, and thus afforded the authors the benefit of a continuing program of research on arc heat-transfer mechanisms.

E-2463

APPENDIX - DATA REDUCTION

The data for run 7 is used here to illustrate numerical procedures of data reduction. Table III lists all pertinent data for each run.

Table III. - Reduced Data for All Runs

Variable	Run							
	1	2	3	4	5	6	7	8
q_E	24.3	32	33.2	43.5	25.5	25.6	28.2	26.8
q_ϵ	8.4	11.5	11.5	10	10.6	10.5	11.1	12.2
$q_{R,air}$	4.5	5.6	1.8	6.1	5.3	7.0	5.5	5.6
$q_{R,room}$	11.2	17.9	17.5	15	20.2	21	21.1	15.5
$q_{R,E}$	3.4	5	4.1	4.5	5.5	6	5.7	4.5
q_N	74.5	68.3	81.2	90.2	82.9	81.6	89	83.4
q_{CV}	1.1	1.1	1.1	1.1	1.1	1.1	1.1	1.1
$\sum$ q, kw	127.4	141.4	150.2	170.4	151.1	152.8	161.7	149.1
E_A, volts	262	252	276	280	287	287	287	283
I_A, amp	481	590	546	546	568	568	568	590
P_A, kw	126	149	150	163	163	163	163	167

Arc Power

The electrical power input to the arc was calculated from the meter readings of current and voltage:

$$E_A = 287 \text{ v}$$

$$I_A = 568 \text{ amp}$$

$$P_A = 163 \text{ kw}$$

Electrode Cooling

Anode and cathode cooling losses were calculated from measured values of cooling water flow rates and temperature rises:

Anode:

$$q_1 = wc_p(t_2 - t_1) = 1.19 \times 1 \times 10 = 11.9 \text{ Btu/sec}$$

Cathode:

$$q_2 = 1.24 \times 1 \times 12 = 14.9 \text{ Btu/sec}$$

$$q_E = 28.2 \text{ kw}$$

Conduction

The heat transferred by conduction from the inner quartz tube was calculated from the measured flow rate and temperature rise of the unseeded air stream:

$$q_C = 0.095 \times 0.25 \times (520 - 76)$$

$$q_C = 11.1 \text{ kw}$$

Radiation From Arc

The radiation absorbed by the seeded air stream was calculated from the measured flow rate and the increase in the outlet temperature resulting from the addition of carbon particles:

$$q_{R,air} = 0.095 \times 0.25 \times (740 - 520)$$

$$q_{R,air} = 5.5 \text{ kw}$$

The radiant energy transmitted through the seeded air to the room was calculated from the heat absorbed by the air and the particle transmissivity calculated from the measured radiant intensity with and without seeding, R' and R respectively:

$$I/I_o = \text{fraction transmitted} = R'/R = 1.15/1.45$$

$$I - I/I_o = \text{fraction absorbed} = 1 - 0.792 = 0.208$$

$$q_{R,room} = 5.5 \times 0.792/0.208 = 21.1 \text{ kw}$$

The total radiation released within the heat exchanger is then:

$$q_{R,HX} = 26.6 \text{ kw}$$

Nitrogen Enthalpy Rise

The nitrogen outlet temperature and enthalpy rise was calculated from the measured nitrogen flow rate and inlet temperature, and the flow rate and temperature of the nitrogen-air mixture entering the exhaust collector:

$$w_N = 0.0504 \text{ lb/sec} \qquad t_{N,1} = 530^\circ \text{ R} \qquad c_{p,N} = 0.3 \text{ Btu/lb-}^\circ\text{F}$$

$$w_{mix} = 0.206 \text{ lb/sec} \qquad t_{1,air} = 530^\circ \text{ R} \qquad t_{mix} = 2120^\circ \text{ R} \qquad c_{p,air} = 0.245$$

A heat-balance calculation on the nitrogen and air mixing process then gives:

$$t_{N,2} = 6120^{\circ} \text{ R}$$

$$q_N = 89 \text{ kw}$$

The outlet nitrogen temperature thus obtained is an average exhaust temperature. The temperature of the central arc region is, of course, much higher.

Arc Radiation Beyond End of Heat Exchanger

The radiation emitted from the inner tube and exposed arc that extend beyond the end of the heat exchanger was calculated by assuming the radiation per unit length of the arc to be constant. Thus, the additional 1 inch of quartz tube and 2 inches of bare arc radiate an additional:

$$q_{R,E} = 26.6 \times 3/14 = 5.7 \text{ kw}$$

This gives the total radiation from the arc as:

$$q_R = q_{R,HX} + q_{R,E} = 32.3 \text{ kw}$$

Free Convection From Heat Exchanger to Ambient Air

The convection loss from the outer surface of the heat exchanger to the room was first estimated as free convection from a horizontal pipe in air (ref. 20, p. 241). For an outer surface temperature of 800° F and an air temperature of 76° F, this loss is 0.4 kilowatt. The actual convective heat loss was probably somewhat higher than this value due to air motion induced by the cooling tubes (see fig. 2). For an assumed air velocity of 10 feet per second, the heat loss calculated from data for air flow normal to single cylinders (ref. 20, p. 221) is

$$q_{CV} = 1.1 \text{ kw}$$

This was felt to be a more realistic estimate and was used as the convective loss for all runs.

REFERENCES

1. Deissler, Robert G.: Diffusion Approximation for Thermal Radiation in Gases with Jump Boundary Condition. ASME paper 63-HT-13 (To be pub. in Jour. Heat Transfer).

2. Howell, John R.: Determination of Combined Conduction and Radiation of Heat Through Absorbing Media by the Exchange-Factor Approximation. To be presented at AIChE-ASME Seventh Nat. Heat Transf. Conf., Cleveland (Ohio), 1964.

3. Viskanta, Raymond: Interaction of Heat Transfer by Conduction, Convection, and Radiation in a Radiating Fluid. ASME Jour. Heat Transfer, vol. 85, ser. C, 1963, pp. 318-328.

4. Viskanta, Raymond, and Grosh, Richard J.: Effect of Surface Emissivity on Heat Transfer by Simultaneous Conduction and Radiation. Int. Jour. Heat and Mass Transfer, vol. 5, 1962, pp. 729-734.

5. Howell, John R., and Perlmutter, M.: Monte Carlo Solution of Radiant Heat Transfer in a Nongrey Nonisothermal Gas with Temperature-Dependent Properties. AIChE paper 6051, 1963.

6. Einstein, Thomas H.: Radiant Heat Transfer to Absorbing Gases Enclosed Between Parallel Flat Plates with Flow and Conduction. NASA TR R-154, 1963.

7. Einstein, Thomas H.: Radiant Heat Transfer to Absorbing Gases Enclosed in a Circular Pipe with Conduction, Gas Flow, and Internal Heat Generation. NASA TR R-156, 1963.

8. Ragsdale, Robert G., and Einstein, Thomas H.: Two-Dimensional Gray-Gas Radiant Heat Transfer in a Coaxial-Flow Gaseous Reactor. NASA TN D-2124, 1964.

9. Anon.: Ninth Symposium (International) on Combustion, 1962 Academic Press, 1963.

10. Tien, C. L.: Heat Transfer by a Turbulently Flowing Fluid-Solids Mixture in a Pipe. ASME Jour. Heat Transfer, vol. 183, 1961, pp. 183-188.

11. Johnstone, H. F., Pigford, R. L., and Chapin, J. H.: Heat Transfer to Clouds of Falling Particles. AIChE, vol. 37, 1941, pp. 95-133.

12. Lanzo, Chester D., and Ragsdale, Robert G.: Experimental Determination of Spectral and Total Transmissivities of Clouds of Small Particles. NASA TN D-1405, 1962.

13. Stull, V. R., and Plass, G. N.: Emissivity of Dispersed Carbon Particles. Jour. Opt. Soc. Amer., vol. 50, 1960, pp. 121-129.

14. Barré, J. J.: Proc. Eighth Int. Astro. Cong., Barcelona, 1957, pp. 1-14.

15. Marble, Frank E.: Dynamics of a Gas Containing Small Solid Particles. In: Combustion and Propulsion, Pergamon Press, 1963, pp. 175-213.

16. Torobin, L. B., and Gauvin, W. H.: Solids-Gas Flow. Part V. The Effects of Fluid Turbulence on Particle Drag Coefficient. Can. Jour. Chem. Eng., vol. 38, Dec. 1960, pp. 189-200.

17. Andrada, T., and Erfurth, K. A.: An Experimental Investigation of a Vortex-Stabilized Long Alternating Current Arc Discharge. In: Proc. of First Plasma Arc Seminar, ARL 63-151, Sept. 1963, pp. 100-144.

18. Finkelnburg, Wolfgang: The High Current Carbon Arc and Its Mechanism. Jour. App. Phy., vol. 20, 1949, pp. 468-474.

19. Schreiber, Paul W.: Radiation From an Alternating Current Arc. In: Proc. of First Plasma Arc Seminar, ARL 63-151, Sept. 1963, pp. 388-445.

20. McAdams, William H.: Heat Transmission. Second ed., McGraw-Hill Book Col, Inc., 1942.

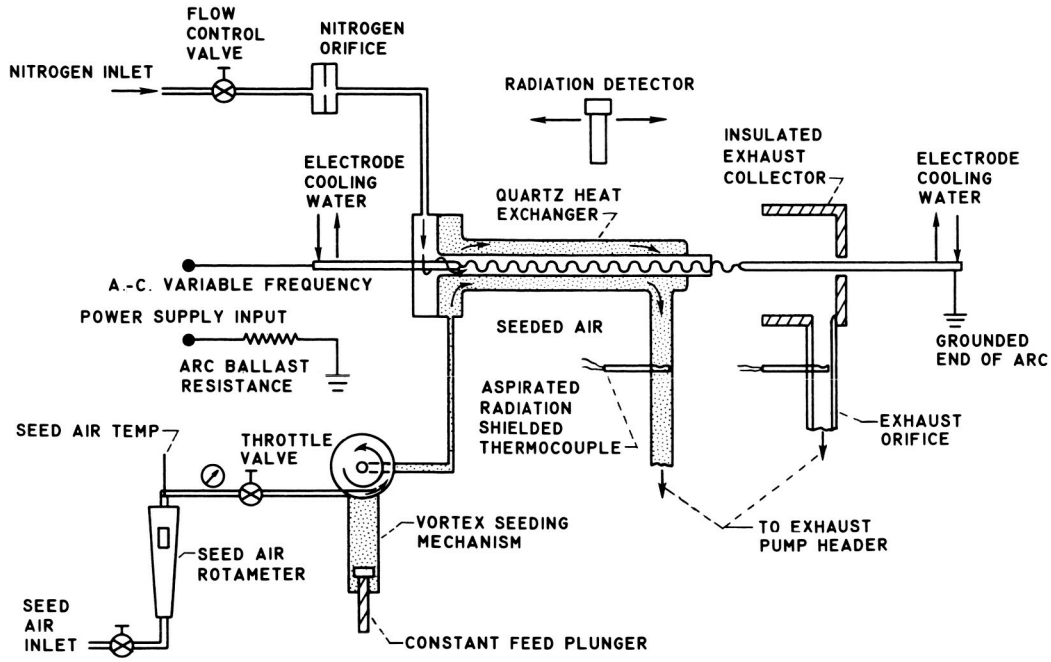

Figure 1. - Experimental apparatus: Schematic drawing of arc and instrumentation.

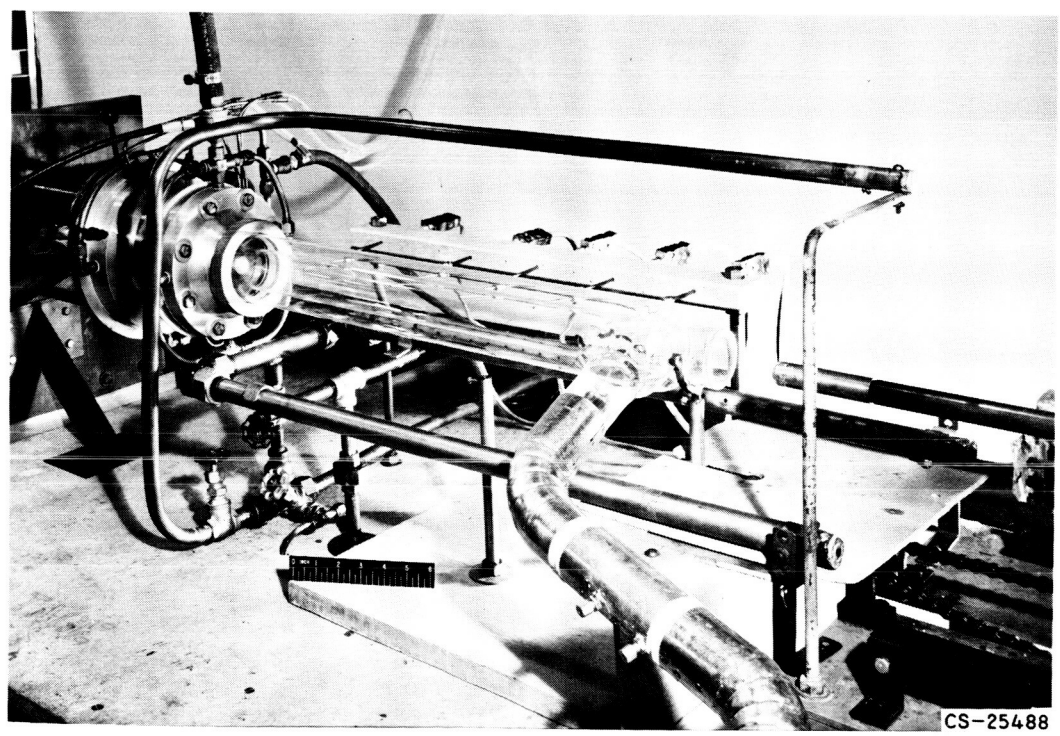

Figure 2. - Transparent heat exchanger.

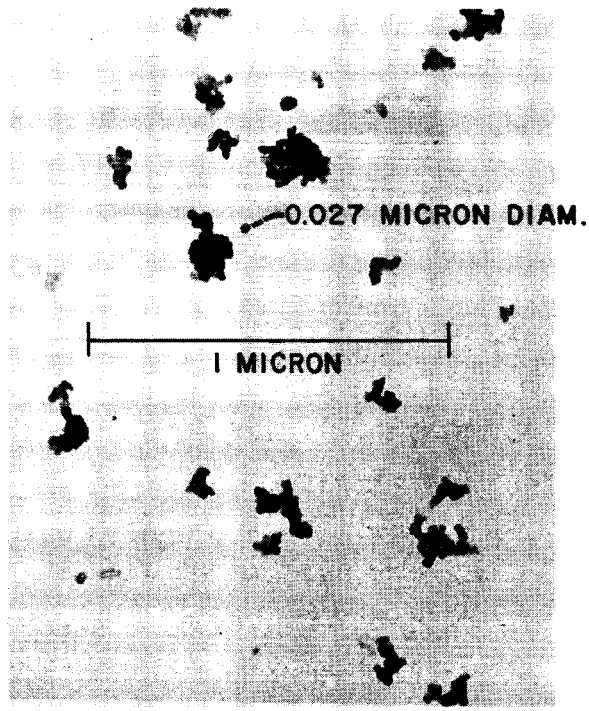

Figure 3. - Electron photomicrograph of carbon particles. 130,800×.

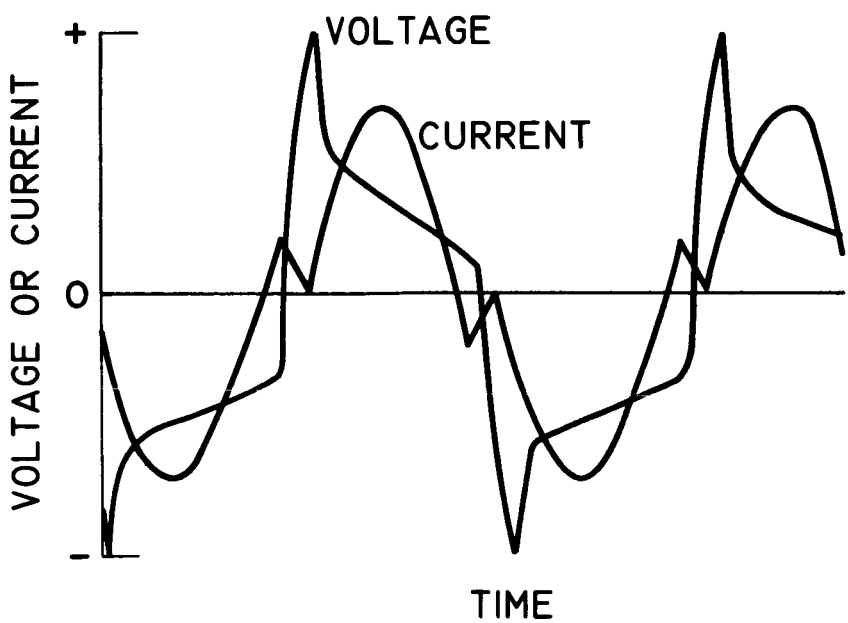

Figure 4. - Arc current-voltage cycle. Current, 525 amperes, voltage, 483 volts; frequency, 24 cycles per second; arc length, 18 inches.

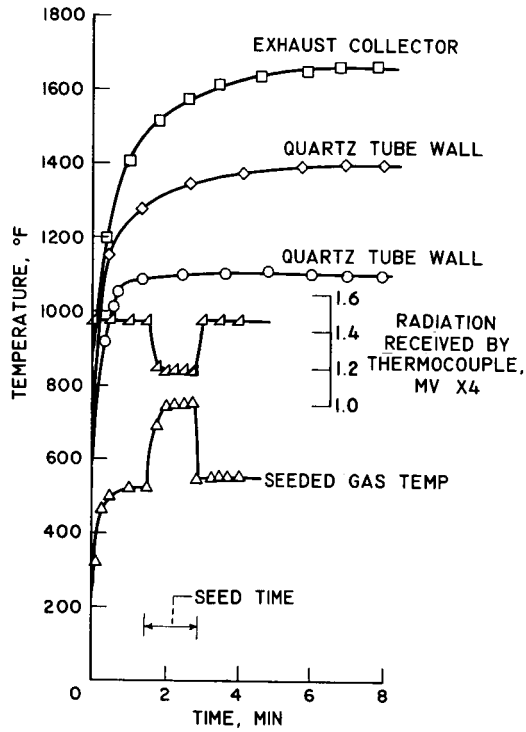

Figure 5. - Heat exchanger transients.

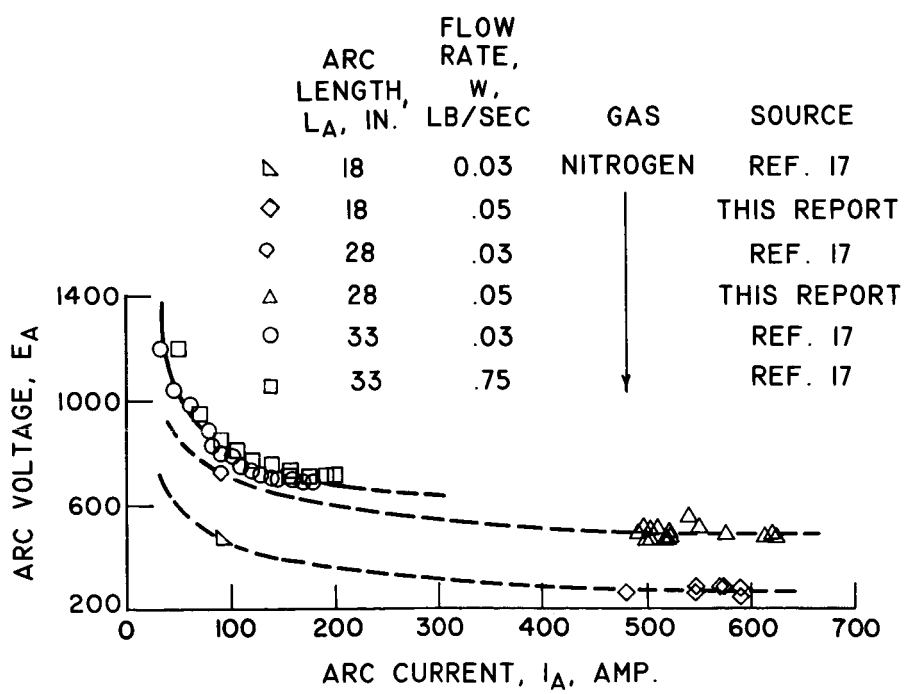

Figure 6. - Arc current-voltage characteristics.

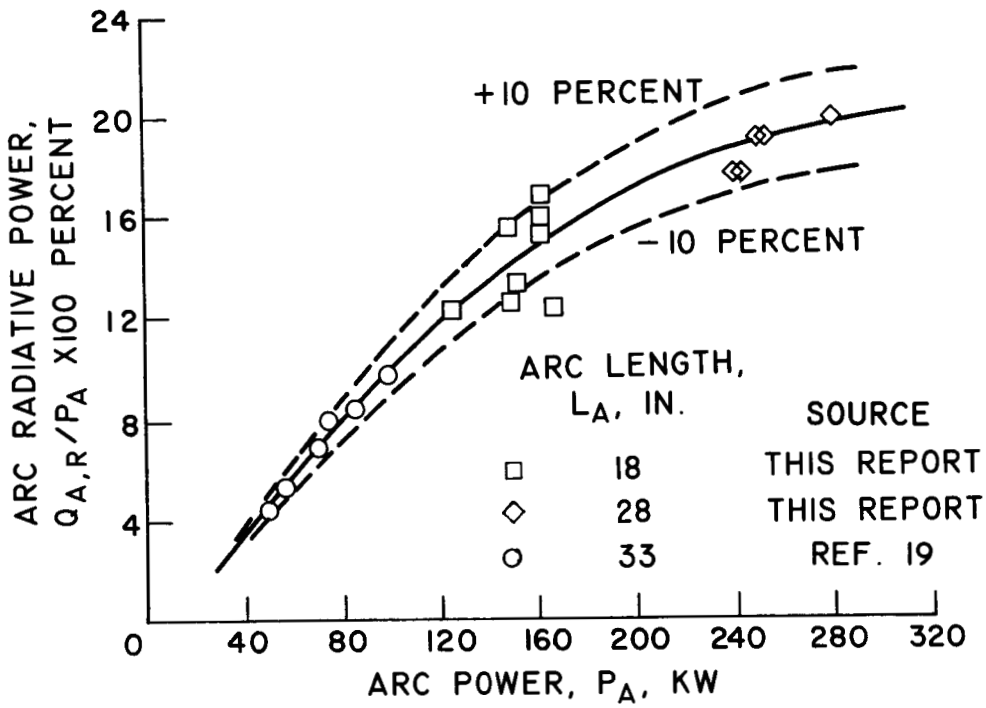

Figure 7. - Effect of power level on arc radiation.

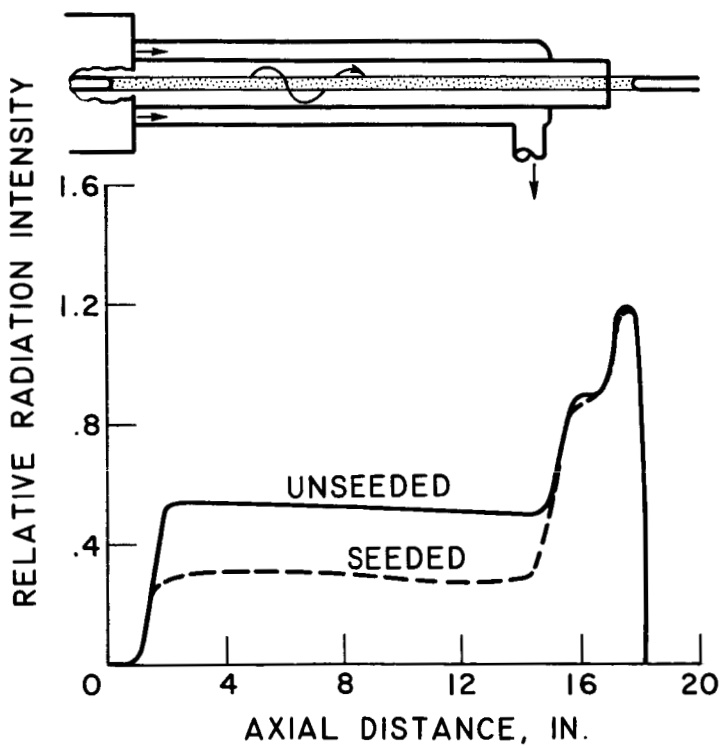

Figure 8. - Axial variation of arc radiant intensity.

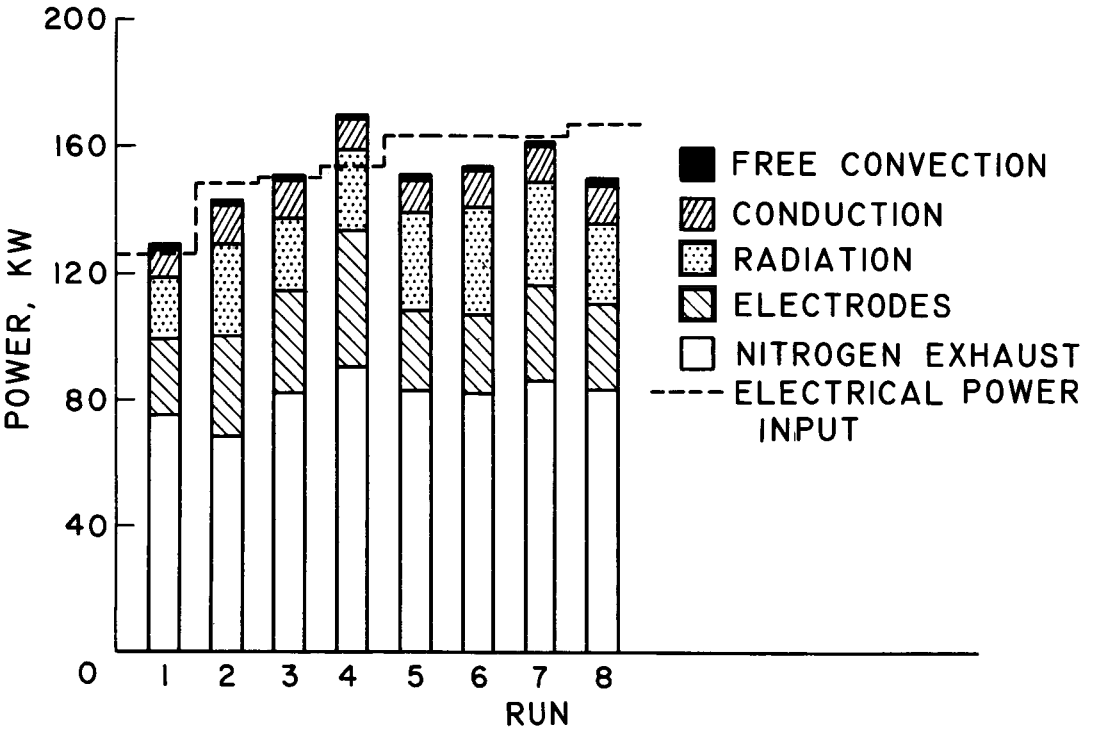

Figure 9. - Arc power distribution.

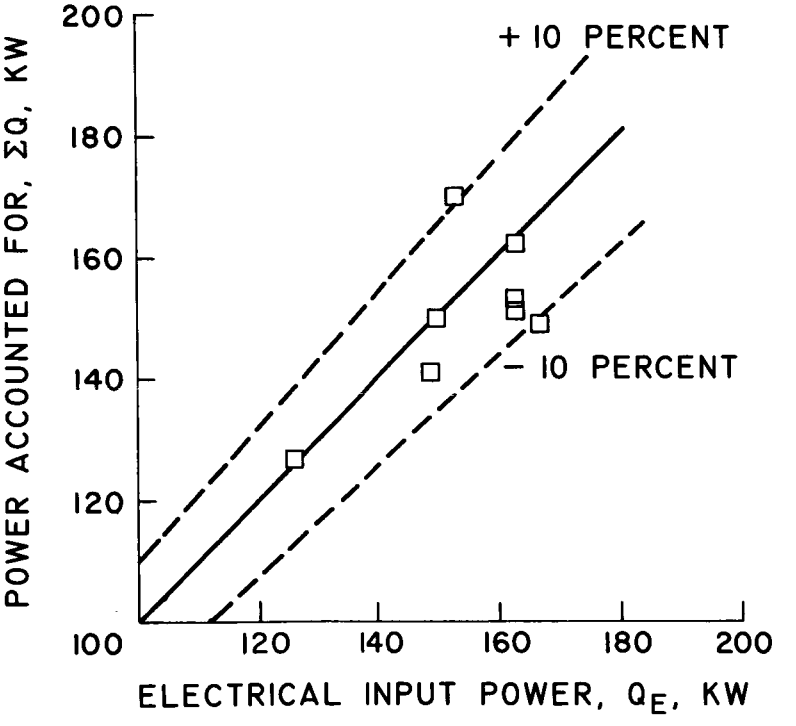

Figure 10. - Heat balance.

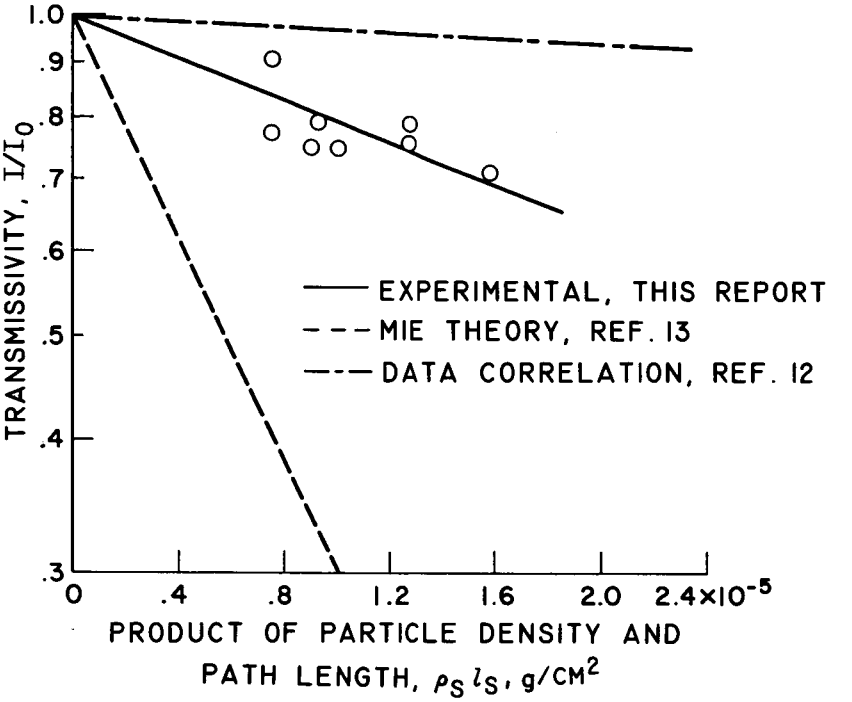

Figure 11. - Transmissivity of 0.027-micron-diameter carbon particles.

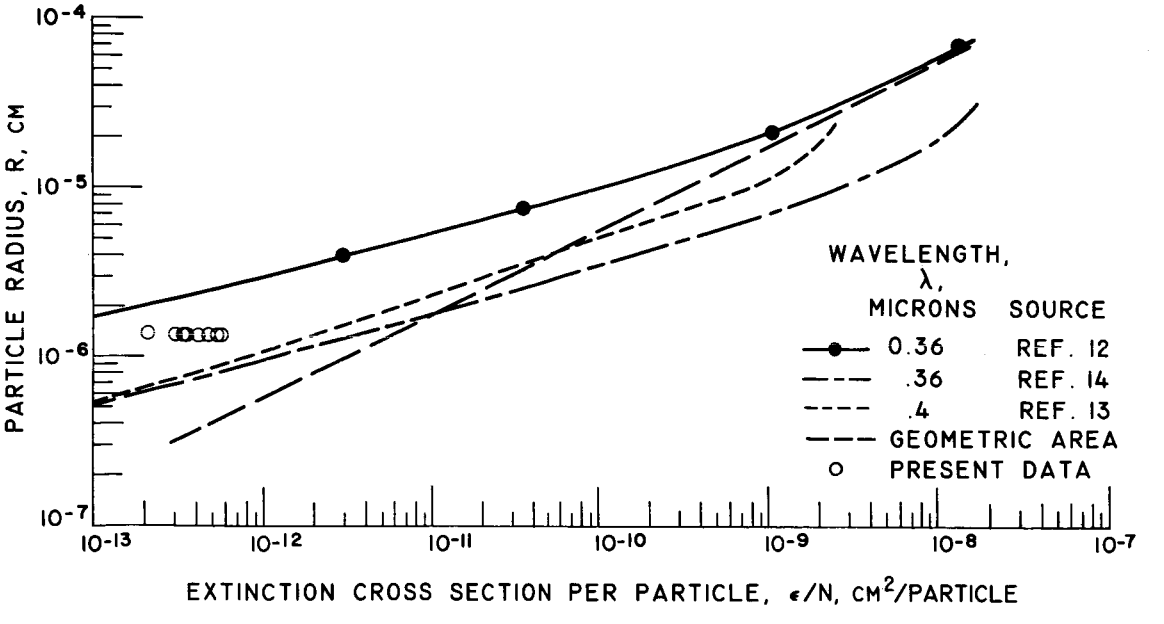

Figure 12. - Extinction cross section per particle of carbon.

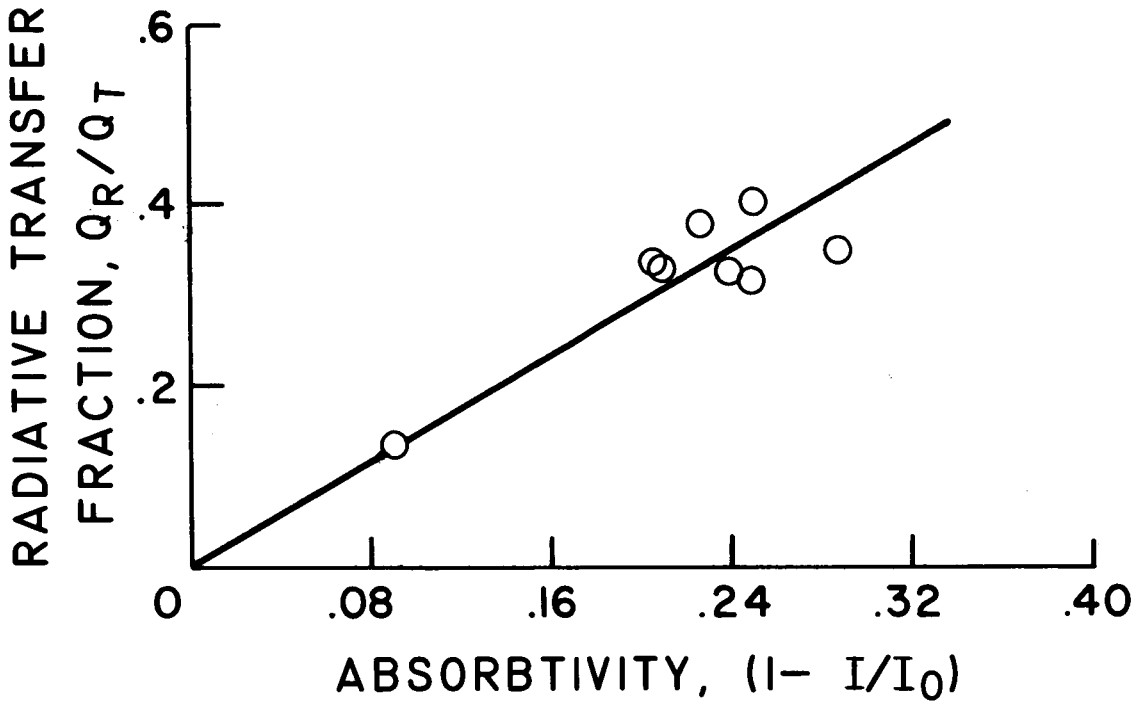

Figure 13. - Effect of particle absorbtivity on fraction of heat transferred as radiation.

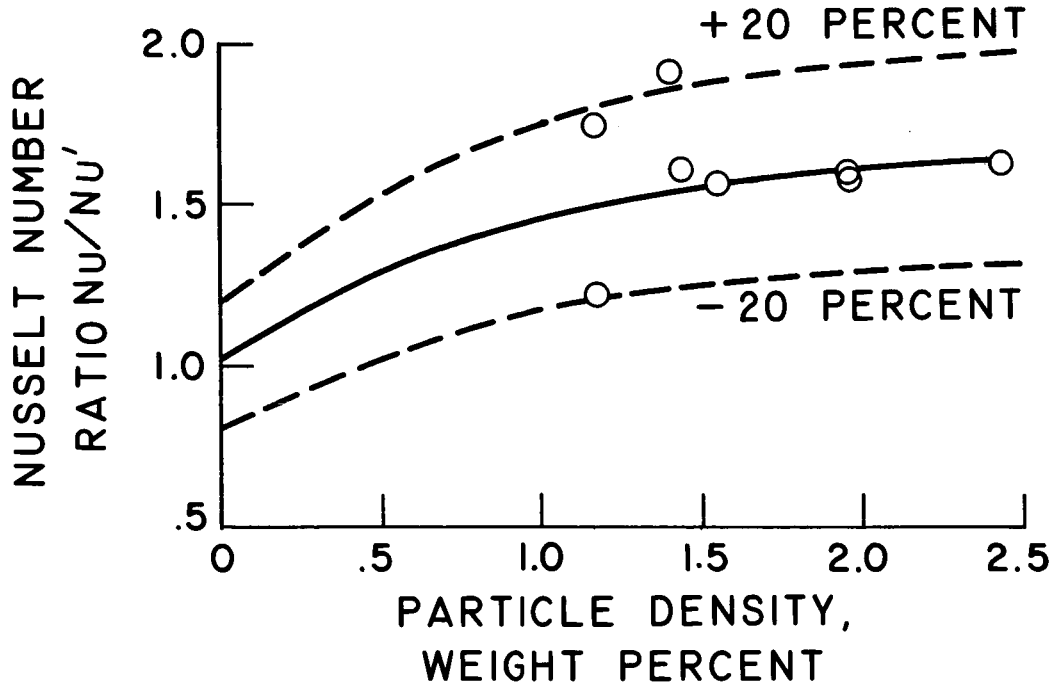

Figure 14. - Effect of particle density on overall heat transfer.